European Review for Medical and Pharmacological Sciences 2017; 21: 4804-4809

Application of dynamic CT to identify lung cancer, pulmonary tuberculosis, and pulmonary inflammatory pseudotumor

X.-L. WANG, W. SHAN

Medical Image Center, The First People's Hospital of Shangqiu, Henan, China

Abstract. – OBJECTIVE: To determine the value of dynamic enhanced computed tomography (CT) scanning in diagnosing lung cancer, pulmonary tuberculosis, and pulmonary inflammatory pseudotumor.

PATIENTS AND METHODS: We recruited 30 patients with pulmonary tuberculoma, 38 with lung cancer, and 16 with pulmonary inflammatory pseudotumor. All patients received CT scanning, dynamic enhanced CT scanning for 20, 30, 45, 60, 75, 90, and 120 s, and scanning for 3, 5, 8, 12, and 15 min. Then, we compared several parameters to determine which ones help with each diagnosis.

RESULTS: The time-density curve for patients with pulmonary tuberculoma was low and flat, and significantly different from lung cancer and inflammatory pseudotumor. The 15 min clearance value and the clearance value for lung cancer and inflammatory pseudotumor were significantly different. The type II time-density curve was common in lung cancer group, whereas the type III time-density curve was common in inflammatory pseudotumor.

CONCLUSIONS: Dynamic enhanced CT scanning demonstrated the ability to differentiate lung cancer, pulmonary tuberculosis, and pulmonary inflammatory pseudotumor, indicating its diagnostic value.

Key Words:
CT, Lung cancer, Tuberculosis, Inflammatory pseudotumor.

Introduction

Lung cancer, pulmonary tuberculoma, and inflammatory pseudotumor are manifested by lesions with nodular appearances in the lung. As the three diseases are characterized by varied morphology and unstable imaging findings, spiral CT of lesions shows overlap with each other, which leads to difficult clinical diagnosis and differential diagnosis. Though CT equipment and image processing technologies are enjoying rapid development, they still lead to some misdiagnosis. So it is necessary to carry out further research on the imaging diagnostics for these three diseases. Here, we applied dynamic enhanced CT to analyze and compare the CT characteristics of lung cancer, pulmonary tuberculoma, and inflammatory pseudotumor after bolus injection of iodine contrast medium through a vein, so that the blood supply features of the three diseases at different periods are reflected. We hope that this study will provide a reference for future clinical diagnosis.

Patients and Methods

Patients

Inclusion criteria: (1) The foci were identified by conventional CT scanning without a definite diagnosis, which required further evaluation. (2) The diameter of the lesion on the mediastinal window was 5-35 mm. (3) Pulmonary tuberculoma, lung cancer, and pulmonary inflammatory pseudotumor were confirmed by surgery and puncture pathology. (4) The patients did not receive radiotherapy, chemotherapy, or molecular targeting treatment. (5) The patients read and signed the informed consent. Exclusion Criteria: (1) Patients did not cooperate holding their breath during scanning. (2) The solid component of the lesion was small or poor from the display of the CT mediastinal window, such as in bronchoalveolar carcinoma. (3) The patients were allergic to the CT enhancement contrast agent iohexol.

The basic clinical information for the patients is summarized in Table I. We enrolled 84 patients, including 47 males and 37 females, with ages ranging 20-78 years old and the average age of 56.4 ± 13.7 years old. 38 patients had lung cancer, including 37 with peripheral lung cancer and 1 with central lung cancer. 18 patients had adenocarcinoma, in-

Corresponding Author: Xing-Long Wang, MD; e-mail: lhnjvvme46@163.com

Table I. Basic clinical information.

	# Cases	Age Mean ± SD	Gender Male	Female	Lesion Location (upper right/middle right/low right/upper left/low left)	Diameter Mean ± SD
Pulmonary tuberculoma	30	53.9 ± 13.5	19	11	(8 / 1 / 6 / 9 / 6)	1.8 ± 0.6
Lung cancer	38	60.7 ± 12.1	22	26	(2 / 4 / 1 6 / 5 / 11)	2.0 ± 0.6
Inflammatory pseudotumor	16	54.6 ± 14.3	6	10	(2 / 2 / 4 / 3 / 5)	2.1 ± 0.7
Total	84	56.4 ± 13.7	47	37	(12 / 7 / 26 /17 / 22)	2.0 ± 0.6

cluding 15 squamous carcinomas, 3 large cell carcinomas, 1 carcinoid, and 1 metastatic tumor. The largest-layer major axis of the transverse, coronal, or sagittal views were selected as lesion diameter. The study was approved by the Ethics Committee of The First People's Hospital of Shangqiu. Signed written informed consents were obtained from all participants before the study.

Computed Tomography (CT)

A 64-layer spiral CT (Somatom Sensation, Siemens, Heusenstamm, Germany) was used for scanning patients. Before scanning, the patients received breath-hold training, to guarantee consistency in the images. Before dynamic enhancement, thin-slice spiral CT scanning was conducted (collimation 1.0 mm, tube voltage 120 kVp, and current 200 mA) to confirm the focus center, with the scanning range from the apex pulmonis to the basis pulmonis. Contrast agent iohexol (370 mg I/mL, Bracco, Milan, Italy) was injected with a high-pressure injector of bolus, with injection flow velocity of 4 mL/s, and a dose of 400 mg/kg calculated by patient weight. Dynamic scanning was conducted to lesion center layer at 20, 30, 45, 60, 75, 90, and 120 seconds and 3, 5, 8, 12, and 15 minutes after injection[1,2] with a scanning interval of 3-4 seconds. After completing the scanning, 20 ml of normal saline was injected at the same rate. All images were recreated by canonical algorithm, resulting in layer thickness of 3 mm. Two regions of interest were selected from the mediastinal window to avoid macroscopic necrosis, cystic change, and calcification areas. The average value was selected as the CT value of this measurement, and each lesion was measured 12 times. Aorta CT value was measured on the same layer of focus center layer.

Observation Indexes

For the three groups of patient, we collected the difference of Peak value (PHU), time to peak, maximum enhancement increase value (ΔHUmax), the ratio of CT value of lesion and aorta CT of the same layer (ΔHUmax/AHU, %), 15 min clearance value, and 15 min clearance rate (15 min clearance value / maximum enhancement increase value x 100%). We analyzed the features of the time-density curves for each group[1]. The time-density curve for pulmonary nodule dynamic enhancement was divided into 4 types to count the node number of each curve type. Type I: enhancement net added value < 20 HU; type II: enhancement net added value > 20 HU, clearance value 5-31 HU; type III: enhancement net added value ≥ 20 HU, clearance value >31 HU; and type IV: enhancement net added value ≥ 20 HU, with continuous enhancement (clearance value < 5 HU).

Statistical Analysis

Data were analyzed with the statistical software SPSS18.0 (SPSS Inc., Chicago, IL, USA). The Kolmogorov-Smirnov method was applied to normality test, and the measurement data that met normal distribution were expressed as mean ± standard deviation. Homogeneity test of variance was used to analyze the difference of each index between the three groups. The measurement data that did not conform to normal distribution were expressed as median (quartile number of lag), and Kruskal-Wallis H was applied to test and analyze the index difference between the three groups. Chi-square test was used to calculate the differences of curve type constituent ratio, and $p<0.05$ meant that the difference was statistically significant.

Results

Baseline Clinical Information

We analyzed the baseline clinical information for the patients. We found no significant differences in age composition (F=3.672, p=0.417) and

Table II. Observation indexes on CT images.

	Tuberculoma	Lung Cancer	Inflammatory Pseudotumor	
Plain CT value (Scope, HU)	28.42 ± 10.43 (16.2-43.7)	29.31 ± 9.87 (23.6-54.7)	27.54 ± 10.2 (21.3-56.2)	$p > 0.05$
PHU (Scope, HU)	35.92 ± 7.58 (18.3-57.3)	79.25 ± 13.47 (36.3-127.4)	86.82 ± 13.24 (37.6-134.3)	$^{*}p > 0.05$
ΔHUmax (Scope, HU)	6.5 ± 10.45 (2.1-13.6)	49.8 ± 12.45 (12.7-72.7)	58.32 ± 14.56 (16.3-78.1)	$^{*}p > 0.05$
ΔHUmax/AHU (%)	6.0 ± 6.75	18.6 ± 7.35	17.4 ± 9.56	$^{*}p > 0.05$
15 min clearance value	5.25 ± 3.32	46.07 ± 4.064	32.06 ± 2.26	$^{\#}p > 0.05$
15 min clearance rate	4.5 ± 12.3	17.8 ± 14.5	34.5 ± 24.5	$^{\#}p < 0.05$

Note: besides plain scanning CT value, the value of tuberculoma was less than that of lung cancer and inflammatory pseudotumor, therefore *meant the independent-sample T test of lung cancer and inflammatory pseudotumor and $^{\#}$stood for p value from Mann-Whitney detection.

gender composition (χ^2=3.467, p=0.177) for the three groups (Table I). The diameter of the lesions also had no significant differences (F=1.483, p=0.356).

Time-Density Curves

The time-density curve for patient with pulmonary tuberculoma was low and flat, with enhancement peak value of 35.92 ± 7.58 HU, scope of 18.3-57.3 HU, maximum enhancement increase value of 6.5 ±10.45 HU, most non-enhancement (17/30) or mild enhancement (11/30). Two cases exhibited ring-enhancement with thin tuberculoma wall, smooth inner wall, and uneven ektexine (Table II).

The general trend of the time-density curve for the lung cancer and inflammatory pseudotumor groups are shown in Figure 1. The peak value for the lung cancer group was 79.25 ± 13.47 HU, with scope of 36.3-127.4 HU, and 18 cases sowed peak time within 30-60 s, 10 within 60-90 s, 5 within 90-120 s, 3 above 120 s, with an average peak value of 66.61±27.26 s (Table II). In the inflammatory pseudotumor group, 5 cases had peak time within 30-60 s, 6 within 60-90 s, 3 within 90-120 s, 2 above 120 s, with an average peak value of 71.63 ± 23.64 s (Table II). We found no significant differences (t=0.641, p=0.524). When lesion enhancement reached peak value, scanning continued, and CT values of the two groups showed a declining trend.

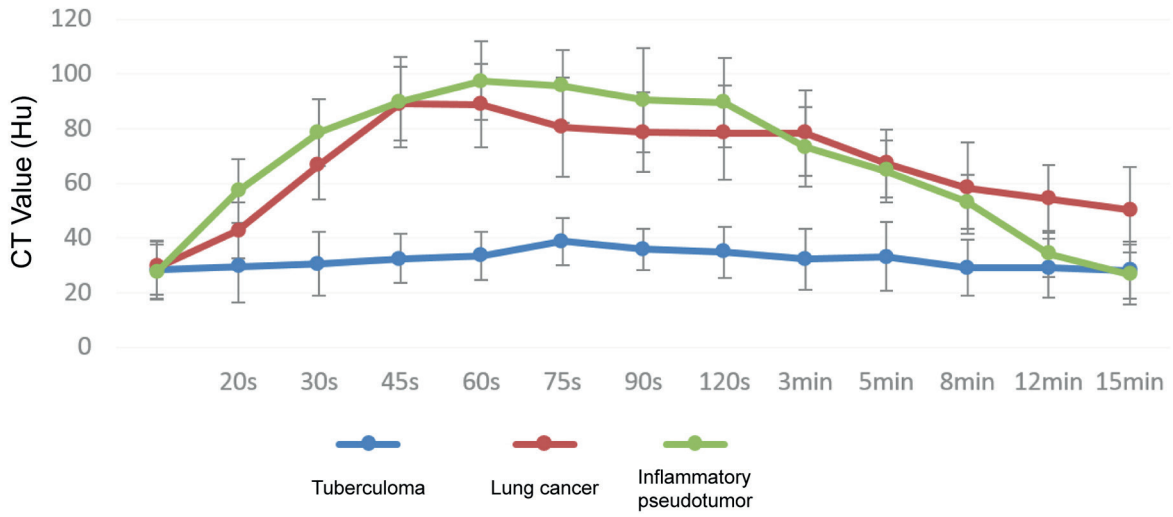

Figure 1. The general trend of the time-density curve for tuberculoma, lung cancer and inflammatory pseudotumor.

Table III. Curve types for lung cancer and inflammatory pseudotumor.

Curve Types	Lung Cancer	Inflammatory Pseudotumor	
I	4	3	$p > 0.05$
II	21	3	$p < 0.05$
III	6	7	$p < 0.05$
IV	7	3	$p > 0.05$

Comparison of Statistical Indexes

We next compared statistical indexes over CT images for the three groups (Figure 2). The plain scanning CT value for the three groups showed no significant differences (F=1.374, $p>0.05$). After injecting contrast agent, peak value, the ratio and maximum enhancement value and aorta enhancement value of the same layer (ΔHUmax/AHU), maximum enhancement increase value (ΔHUmax), 15 min clearance value, and 15 min clearance rate were lower in the tuberculoma group than in the lung cancer and inflammatory pseudotumor groups. Also, the time-density curve for the tuberculoma group was low and flat. Therefore, the above-mentioned indexes for the lung cancer and inflammatory pseudotumor groups were analyzed with independent-sample *t*-test. The 15 min clearance value (Z=-2.899, p=0.004) and 15 min clearance rate (Z=-1.376, p=0.000) for the lung cancer and inflammatory pseudotumor groups had significant differences, but other indexes showed no significant differences.

The most common curve type for lung cancer was the type II, with enhancement net added value I >20 HU, clearance value 5-31 HU, and total number of 21 cases, accounting for 55.3% (21/38). The most common curve type for inflammatory pseudotumor was the type III, with enhancement net added value ≥20 HU, clearance value >31 HU, accounting for 43.8% (7/16). Type I curve accounted for 10.5% (4/38) in lung cancer and 18.7% (3/16) in inflammatory pseudotumor. Type IV curve accounted for 18.4% (7/38) in lung cancer and 18.7% (3/16) in inflammatory pseudotumor.

Discussion

In recent years, many scholars at home and abroad have explored the utility of dynamic enhancement CT to identify benign and malignant solitary pulmonary nodules[3-6]. However little research has been done on the application of dynamic enhancement CT to identify tuberculoma, lung cancer, and inflammatory pseudotumor. Feng et al[7] analyzed and reported the features of 44 cases with pulmonary tuberculoma, lung cancer, and inflammatory pseudotumor displayed

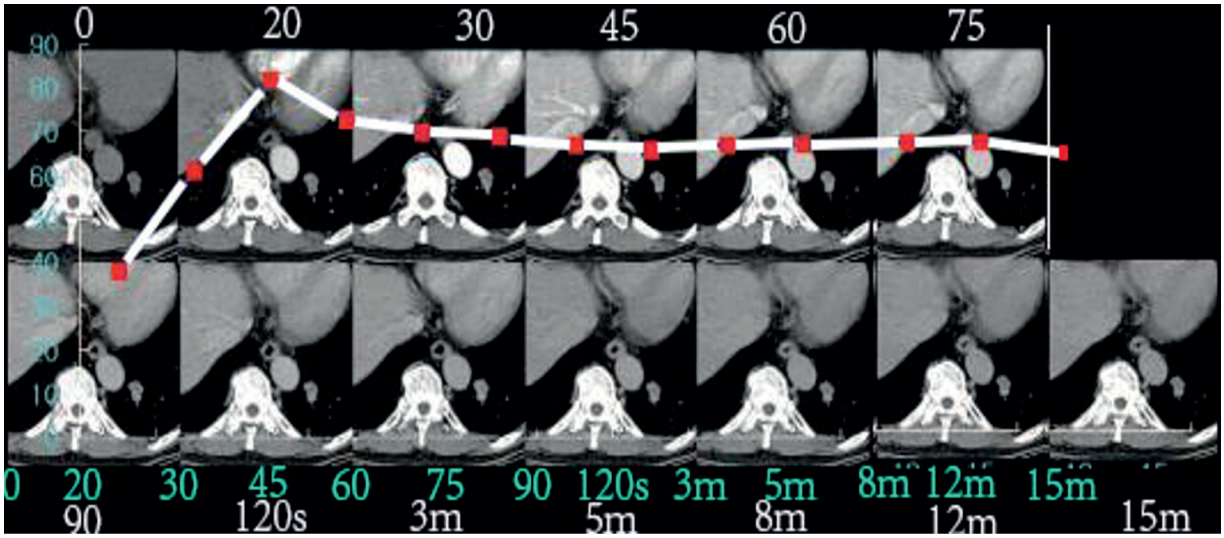

Figure 2. Enhanced CT images for a case with lung adenocarcinoma.

on dynamic enhancement CT scanning images. Most of them were case studies that described the lesion features but were not analyzed statistically. Shenjiang et al[8] was the only to study dynamic enhancement scanning for 15 min. This case study conducted statistical analysis and researched image features, which was of great innovation.

Pulmonary tuberculoma, lung cancer, and inflammatory pseudotumor are common in solitary pulmonary nodules. Their form is similar in high-resolution CT, and the CT value of soft-tissue window by plain scanning is also close, complicating their identification by conventional pulmonary CT. In this study, the CT value for three groups of patients by plain scanning showed no significant difference. After injection of contrast agent, tuberculoma often contained caseous necrosis material, with non-enhancement of 56.7% (17/30) or mild enhancement of 36.7% (11/30). Two cases presented with ring-enhancement, featuring even thin-wall enhancement and smooth inner wall, which was related to the envelope of the tuberculoma. The envelope of the tuberculoma can be divided into two layers, and the inner layer tuberculous granulation tissue that contains vascular structure[9], so dynamic enhancement scanning can be intensified, with a low and flat time-density curse, and enhancement peak value and maximum enhancement increase value were less than that of lung cancer and inflammatory pseudotumor group.

Yi et al[10,11] divided 119 cases of lung nodules into benign and malignant groups. The benign group included many types of lung cancer, and the malignant group included inflammatory pseudotumor. They found significant differences in enhancement peak value and maximum enhancement increase value between the two groups. In our study, the time-density curve overlapped for the lung cancer and inflammatory pseudotumor groups. Additionally, the enhancement peak value and maximum enhancement increase value were comparable between these two groups. Peak value and the ratio of maximum enhancement increase value and aorta had no significant differences either.

Many scholars have explored the value of dynamic enhancement CT value to identify lung cancer and inflammatory pseudotumor. According to Yi et al[10], the time-density curve for peripheral lung cancer overlaps with that of inflammatory pseudotumor. The time of dynamic enhancement scanning was limited to 4 min, so the observation and research after 4 min was lacking. Our study referred to the literature[1,2], to shorten the interval of dynamic enhancement scanning time and prolong the total time to 15 min, so that the capillaries permeation can be observed more carefully. We found that the 15 min clearance value and 15 min clearance rate for the two groups had significant differences, which was similar to other studies[12-14]. The enhancement level of solitary pulmonary nodules had a remarkable correlation with microvessel density[15,16], which depends on the retention level of the contrast agent in the intra- and extravascular mesenchyme[17,18]. During the formation of inflammatory nodules, the pulmonary artery presents with a diffusible thrombus, and the blood supply derives directly from the bronchial artery. The contrast agent enters the blood vessel mesenchyme through a relatively straight blood vessel with a normal structure. The lymphatic drainage of the perivascular space is smooth, so the contrast agent drainage speeds up. Therefore, during dynamic enhancement scanning, the time-density for inflammatory pseudotumor reached the peak value and then dropped, with complete clearance[19]. Lung cancer has a rich blood supply, not only the number and size of bronchial artery increases by 20-30% but also significant changes occur such as expansion, spread, and tortuosity. The reduction or deficiency of lymphatic drainage leads to prolong the time of contrast agent retention. Moreover, the differentiation of tumor angiogenesis is immature and the vessel distribution is chaotic, with large endothelial cell space and incomplete basal membrane, so the permeability of vessel wall is high. Macromolecular contrast agent penetrates easily into the extravascular extracellular space. Furthermore, partial lung cancer capillaries show pool-shape expansion, which favors the retention of the contrast agent[20]. In addition, clearance of the contrast agent is associated with the fibrosis degree of the tumor. The fibrosis degree of malignant tumor is high, so the clearance of the contrast agent is more difficult because fiber tissue is short of blood vessel and lymphatic drainage[21-24]. For this, the 15 min clearance value and 15 min clearance rate for lung cancer and inflammatory pseudotumor were significantly different.

Conclusions

Dynamic enhanced CT scanning demonstrated the ability to differentiate lung cancer, pulmonary tuberculosis, and pulmonary inflammatory pseudotumor, indicating its diagnostic value.

Conflict of interest

The authors declare no conflicts of interest.

References

1) Jeong YJ, Lee KS, Jeong SY, Chung MJ, Shim SS, Kim H, Kwon OJ, Kim S. Solitary pulmonary nodule: characterization with combined wash-in and washout features at dynamic multi-detector row CT. Radiology 2005; 2372: 675-683.
2) Ye XD, Yuan Z, Ye JD, Li HM, Xiao XS. Dynamic enhanced CT evaluation of solitary pulmonary nodules. Zhonghua Zhong Liu Za Zhi 2011; V33N4: 308-312.
3) Ye XD, Ye JD, Yuan Z, Li WT, Xiao XS. Dynamic CT of solitary pulmonary nodules: comparison of contrast medium distribution characteristic of malignant and benign lesions. Clin Transl Oncol 2014; 161: 49-56.
4) Linning E, Wu S, Wang K, Meng H, Sun D, Wu Z. Computed tomography quantitative analysis of components: a new method monitoring the growth of pulmonary nodule. Acta Radiol 2013; 548: 904-908.
5) Chae EJ, Song JW, Krauss B, Song KS, Lee CW, Lee HJ, Seo JB. Dual-energy computed tomography characterization of solitary pulmonary nodules. J Thorac Imaging 2010; 25; 4: 301-310.
6) Ohno Y, Nishio M, Koyama H, Miura S, Yoshikawa T, Matsumoto S, Sugimura K. Dynamic contrast-enhanced CT and MRI for pulmonary nodule assessment. AJR Am J Roentgenol 2014; 2023: 515-529.
7) Feng ST, Chen JD, Meng QF, Yang XF, Xie HB, Yan CG. Imaging features of lung carcinoma, pulmonary tuberculoma, and inflammatory pseudotumor on helical incremental dynamic CT scan--A report of 44 cases. Ai Zheng 2006; 25; 3: 348-351.
8) Shenjiang LI, Xiao X, Huimin LI. Evaluation of blood flow pattern of solitary pulmonary nodules with dynamic enhanced multi-slice spiral CT scanning. J Clin Radiol 2003; 6: 18-21.
9) Totanarungroj K, Chaopotong S, Tongdee T. Distinguishing small primary lung cancer from pulmonary tuberculoma using 64-slices multidetector CT. J Med Assoc Thai 2012; 95: 574-582.
10) Yi CA, Lee KS, Kim EA, Han J, Kim H, Kwon OJ, Jeong YJ, Kim S. Solitary pulmonary nodules: dynamic enhanced multi-detector row CT study and comparison with vascular endothelial growth factor and microvessel density. Radiology 2004; 233: 191-199.
11) Yi CA, Lee KS, Kim BT, Choi JY, Kwon OJ, Kim H, Shim YM, Chung MJ. Tissue characterization of solitary pulmonary nodule: comparative study between helical dynamic CT and integrated PET/CT. J Nucl Med 2006; 47: 443-450.
12) Gao PY, XU BZ. Application value of multislice spiral dynamic contrast-enhanced CT scan in solitary pulmonary nodule. J Clin Pulmon Med 2013; 18: 1483-1484.
13) Bayraktaroglu S, Savas R, Basoglu OK, Cakan A, Mogulkoc N, Cagirici U, Alper H. Dynamic computed tomography in solitary pulmonary nodules. J Comput Assist Tomogr 2008; 32: 222-227.
14) Cronin P, Dwamena BA, Kelly AM, Carlos RC. Solitary pulmonary nodules: meta-analytic comparison of cross-sectional imaging modalities for diagnosis of malignancy. Radiology 2008; 246: 772-782.
15) Jiang NC, Han P, Zhou CK, Zheng JL, Shi HS, Xiao J. Dynamic enhancement patterns of solitary pulmonary nodules at multi-detector row CT and correlation with vascular endothelial growth factor and microvessel density. Ai Zheng 2009; 28: 164-169.
16) Bai RJ, Cheng XG, Qu H, Shen BZ, Han MJ, Wu ZH. Solitary pulmonary nodules: comparison of multi-slice computed tomography perfusion study with vascular endothelial growth factor and microvessel density. Chin Med J 2009; 122: 541-547.
17) Wang Y, Liu XG, Liang MZ, Qin PX, Lin YJ, Yi XP. Correlation of early phase contrast enhancement of multi-detector row computed tomography to tumor stroma of nodular solid lung adenocarcinoma. Ai Zheng 2008; 2711: 1190-1196.
18) Liu J, Xiong Z, Hu C, Zhou M, Zhou H, Chen W, Xia Y. Correlation between multi-slice spiral CT pulmonary perfusion imaging and cavity of microvessel in lung cancer. Zhong Nan Da Xue Xue Bao Yi Xue Ban 2010; 35: 1242-1247.
19) Diederich S, Theegarten D, Stamatis G, Luthen RM. Solitary pulmonary nodule with growth and contrast enhancement at CT: inflammatory pseudotumour as an unusual benign cause. Br J Radiol 2006; 79: 76-78.
20) Zhou H, Liu JK, Chen SX, Xiong Z, Lin GQ, Zhou ML, Chen W, Lu H. Correlation of blood flow assessed by CT perfusion imaging and microvascular ultrastructure in non-small cell lung cancer: a preliminary study. Zhonghua Zhong Liu Za Zhi 2013; 353: 193-197.
21) Dahele M, Palma D, Lagerwaard F, Slotman B, Senan S. Radiological changes after stereotactic radiotherapy for stage I lung cancer. J Thorac Oncol 20116; 7: 1221-1228.
22) Ma GF, Zhang RF, Ying KJ, Wang D. Effect evaluation of cisplatin-gemcitabine combination chemotherapy for advanced non-small celllung cancer patients using microarray data. Eur Rev Med Pharmacol Sci 2015; 19: 578-585.
23) Sverzellati N, Guerci L, Randi G, Calabrò E, La Vecchia C, Marchianò A, Pesci A, Zompatori M, Pastorino U. Interstitial lung diseases in a lung cancer screening trial. Eur Respir J 2011; 38: 392-400.
24) Lv YG, Bao JH, Xu DU, Yan QH, Li YJ, Yuan DL, Ma JH. Characteristic analysis of pulmonary ground-glass lesions with the help of 64-slice CT technology.Eur Rev Med Pharmacol Sci 2017; 21: 3212-3217.